Crystal structure and reactivity of YbdL from *Escherichia coli* identify a methionine aminotransferase function ☆

Manuela Dolzan[a], Kenth Johansson[a], Véronique Roig-Zamboni[a], Valérie Campanacci[a], Mariella Tegoni[a], Gunter Schneider[b,*], Christian Cambillau[a,*]

[a] *Architecture et Fonction des Macromolécules Biologiques, UMR 6098, CNRS and Universités d'Aix-Marseille I and II, 31 chemin J. Aiguier, F-13402 Marseille Cedex 20, France*
[b] *Department of Medical Biochemistry and Biophysics, Karolinska Institutet, S-171 77 Stockholm, Sweden*

Received 13 April 2004; revised 16 June 2004; accepted 28 June 2004

Available online 8 July 2004

Edited by Julian Schroeder

Abstract The *ybdL* gene of *Escherichia coli* codes for a protein of unknown function. Sequence analysis showed moderate homology to several vitamin B_6 dependent enzymes, suggesting that it may bind pyridoxal-5′-phosphate. The structure analysis of YbdL to 2.35 A resolution by protein crystallography verifies that it is a PLP dependent enzyme of fold type I, the typical aspartate aminotransferase fold. The active site contains a bound pyridoxal-5′-phosphate, covalently attached to the conserved active site lysine residue Lys236. The pattern of conserved amino acids in the putative substrate binding pocket of the enzyme reveals that it is most closely related to a hyperthermophilic aromatic residue aminotransferase from the archeon *Pyrococcus horikoshii*. Activity tests with 10 amino acids as amino-donors reveal, however, a preference for Met, followed by His and Phe, results which can be rationalized by modelization studies.

Keywords: Pyridoxal-5′-phosphate; Aminotransferase; Structural genomics

1. Introduction

A recent genomic analysis revealed that close to 1.5% of the genes of prokaryotic organisms code for pyridoxal-5′-phosphate dependent enzymes [1]. This large and diverse group of enzymes comprises several fold families [2–4]. So far, five different folds for pyridoxal-5′-phosphate dependent enzymes have been identified, where fold type I typical for most amino transferases [5] is the most common. Fold type II includes tryptophan synthase as the best-known representative [6]. The structure analysis of alanine racemase [7] was the first of a member of fold type III and revealed that the ubiquitous α/β barrel fold can provide a binding site for PLP. The structure of D-amino acid transferase [8], which defined fold type IV, illustrated that the function of PLP enzymes is not strictly related to the fold family, i.e., PLP enzymes with similar functions can have completely different structures. Finally, fold type V is so far only found in vitamin B_6 dependent enzymes that do not use electrophilic catalysis typical of PLP, but rather employ the phosphate group of the cofactor in their mechanisms as for instance in glycogen phosphorylase [9].

Sequence analysis suggests that the majority of PLP enzymes belongs to the fold type I family [10]. In view of the large number of PLP enzymes that belong to this fold family, the coverage of the 3D space is rather scarce: at present, the PDB holds only about 30 structures of different type I PLP enzymes. The enzymes of this family catalyze a large range of chemical reactions and this diversity is also reflected on a structural level. A comparison of the members of this family with known 3D structure revealed that they can be further divided into at least six subclasses, with α-aminotransferases forming subclass I [4,11]. These aminotransferases catalyze amino group transfer between an amino acid and an oxo acid substrate in a reaction, which involves formation of covalently linked intermediates between substrate and the PLP cofactor [12]. The limited structural knowledge of this fold family has already generated significant insights into the structural basis of PLP catalysis, substrate specificity and evolution of PLP enzymes [12]. However, given the diversity in sequence and function, a more extensive structural characterization of this fold family (and of other fold families) appears timely, and in view of available high-throughput technologies also feasible.

We have set-up a medium-scaled structural genomics program aiming at solving the structures of as many *Escherichia coli* unknown ORF products as possible among 110 targets. The rationale for choosing these targets was their wide distribution through the bacterial kingdom, their unknown function ('y' prefix) and an amino acid identity with any protein sequence of known function lower than 30% [13]. The general approach for expression and crystallization of these 110 ORF products has been described elsewhere [14,15].

The *ybdL* gene from *E. coli* shows moderate (<30%) sequence identity to PLP enzymes of known structure and, thus, suggested that it may be a vitamin B_6 dependent enzyme. The structure analysis of YbdL verifies that it is very close to type I class of vitamin B_6 dependent enzymes, and, as expected for this class of enzymes, it binds PLP. A structure-based sequence comparison with other enzymes of this family identifies a glutamic/aromatic aminotransferase from the hyperthermophilic archeon *Pyrococcus horikoshii* [16] as the closest structural relative. The analysis of the pattern of conserved amino

☆ The coordinates have been deposited to the Protein Data Bank at RCSB (http://www.rcsb.org/pdb/) as entry 1U08.

* Corresponding authors. Fax: +46-8-327626 (G. Schneider); fax: +33-491-16-45-36 (C. Cambillau).
E-mail addresses: gunter.schneider@mbb.ki.se (G. Schneider), cambillau@afmb.cnrs-mrs.fr (C. Cambillau).

0014-5793/$22.00
doi:10.1016/j.febslet.2004.06.075

acids in the putative substrate binding site suggested that YbdL might be an aromatic aminotransferase. Activity tests on the first half-reaction with several amino acids revealed, however, a amino-donor preference in the following order Met > His > Phe > Tyr ~ Leu > Glu.

2. Materials and methods

2.1. Cloning of gene and expression vectors

The *YbdL* gene was subcloned into the Gateway system (Invitrogen) [17]. The ORF of interest was amplified by PCR using the whole *E. coli* genome and primers containing the recombination sites at their 5′ end. The sequences of the primers were 5′-ACAAGTTTGTACAAAAAAGCAGGCTTAACAAATAACCCTCTGATTCCA-3′ (forward primer) and 5′-ACCACTTTGTACAAGAAAGCTGGGTCCTAAAGCTGGCGC AGGCGTTC-3′ (reverse primer; the attB sequences are underlined). The PCR product was then subcloned into the shuttle vector (pDONR201 – Invitrogen). At this point, the ORF was directly transferred from the shuttle vector to the pDest17 destination vector. The expression vector pDest17 encodes an His6 tag linked to the N-terminus of the target protein by means of 15 residues encoded by the 5′ recombination site [17]. The resulting fusion protein therefore carried 21 non-native amino acids at its N-terminus. Since a single expression vector was used, the cloning followed the so-called ''one-tube reaction'' protocol. *E. coli* DH5α were transformed with the whole mixture (Gateway BP protocol, see [17]) and recombinant clones were selected by plating on ampicillin plates.

2.2. Overexpression and protein purification

Protein expression was first analyzed in 4-ml cultures, and, if positive, purification was performed using a larger volume. The cloned gene was expressed in the host *E. coli* strain C41 (DE3) according to the manufacturer's instructions (Avidis). Cells were grown at 37 °C in Luria–Bertani medium (Invitrogen) containing 100 μg/ml ampicillin. When the optical density of the culture reached a value of 0.5 at 600 nm, expression was induced by addition of isopropyl-β-D-thiogalactopyranoside to a final concentration of 0.5 mM. The induction time was one night at 25 °C. Purification was performed on a Pharmacia Äkta FPLC. The first purification step was passage through a Ni affinity column. Protein that eluted from the Ni column was further purified by gel filtration on Superdex 200 pg (Amersham Biosciences).

Protein purity and molecular mass were checked by SDS–PAGE and MALDI–TOF mass spectroscopy, respectively. The mono- or oligomeric state of the proteins was determined by dynamic light scattering (DLS) with a DYNAPRO instrument (Protein solutions). Before measurement, the protein was filtered with a Millipore 4 mm syringe unit. The measurement was performed by injecting 15 μl of protein buffered with 5 mM HEPES and 150 mM NaCl, pH 7.5, at ~18 mg/ml. All calculations were carried out using the software provided with the instrument. Four independent measurements of 20 acquisitions were carried out. Apparent molecular mass was deduced from the measurements. The presence of secondary structures was assessed by circular dichroism with a JASCO 800 spectrometer at a protein concentration of 0.1 mg/ml.

2.3. Crystallization, data collection and processing

Crystallization experiments were performed immediately after protein purification. The protein was crystallized using the vapor diffusion method at 20 °C. The nanoliter crystallization experiments were performed using the sitting-drop method in Greiner plates [15]. The reservoirs of the Greiner plates were filled using the TECAN robot, while the nanoliter drops were dispensed by a Cartesian robot. Screening experiments were performed with several commercial kits: Stura Footprint Screen [18] and Structure Screen 1 and 2 [19] purchased from Molecular Dimension Limited (http://www.molecular-dimensions.com), and Wizard Screen I and II purchased from Emerald Bio-Structures (http://www.decode.com/emeraldbiostructures). The screens were set up in 96 well Greiner crystallization plates, with three shelves for each well and each condition was tested at three different protein concentrations. Reservoir solutions were 200 μl in volume and crystallization drops were composed of 100, 200 and 300 nl of protein solution and 100 nl of reservoir solution. At the optimization step, well solutions consisted of 0.2 M NaCl, 0.1 M Na/KPO_4, pH 6.3, and 23.5% w/v PEG1000. Sitting drops were formed by mixing 300, 200 and 100 nl of 9.3 mg/ml protein in 5 mM HEPES and 150 mM NaCl, pH 7.5, and 100 nl of well solutions. Crystals were grown at 20 °C and reached a size of $0.2 \times 0.1 \times 0.1$ mm^3.

Table 1
Data collection and refinement statistics

Data collection	All
Space group	$P2_12_12_1$
Unit cell parameters (Å)	55.4 104.3 168.4
Beamline	ID14-EH2
Temperature (K)	100
Wavelength (Å)	0.933
Number of images	360
Resolution range (Å)[a]	30–2.35 (2.42–2.35)
Number of observations	229150
Unique reflections	37638
Redundancy	6.1 (4.9)
Completeness (%)	91.0 (67.1)
$I/\sigma I$	8.5 (2.7)
R_{sym}(%)	6.4 (22.7)
Refinement	
R/R_{free}(%)	19.9/22.5
Wilson *B* factor	36.5
rmsd bonds length (Å)	0.008
rmsd bonds angles (°)	1.46

[a] Values in parentheses are for the highest resolution shell.

The crystals obtained belong to space group $P2_12_12_1$ with cell dimensions $a = 55.4$ Å, $b = 104.3$ Å and $c = 168.4$ Å. The V_m value is 2.7 Å^3/Da assuming a dimer in the asymmetric unit, corresponding to 54% water content [20]. The diffraction data were collected at 100 K on beamline ID14-EH2 at the European Synchrotron Radiation Facility (Grenoble, France) using a MarCCD detector. Data indexing, scaling and reduction were carried out using DENZO [21] and Scala [22]. Intensity data were collected to a resolution of 2.35 Å. The data collection statistics are reported in Table 1.

2.4. Structure determination and refinement

The structure was solved by molecular replacement using AMoRe [23]. The search model was the structure of an aromatic amino acid aminotransferase (ArATPh) from the hyperthermophilic archaeon *Pyrococcus horikoshii* (Protein Data Bank entry 1DJU) [16], which displays 30% identity with YbdL. The phases were improved by averaging and solvent flattering using DM [22]. Model building was carried out with the program O [24]. The model was refined using CNS [25] and 5% of the unique reflections were used to monitor the progress of the refinement by R_{free} validation. Analysis and inspection of the structures were carried out with the program O [24]. The figures were generated with Molscript [26] and PyMol [27].

2.5. Reactivity study

The first amino-transfer reaction (see scheme, section 3–5) was assessed spectophotometrically (using a Varian Cary Spectrometer) following the decrease of the E-PLP absorption at 430 nm (main band) and, as a check, the increase of the E-PMP absorption at 327 nm. The enzyme was from a single batch, concentrated at 8 μM, and contained one equivalent of naturally occurring PLP bound in the active site. Amino acids, purchased from Sigma–Aldrich (see list in Table 2), were added at a concentration of 1 or 0.1 mM (Met, His). The reaction was followed at 430 nm for 2 min; spectra were recorded before the addition of the amino acid and 1 min after the end of the kinetic.

Table 2
Reactivity of YbdL with 10 amino acids in the first reaction (amino-donor) measured as the % of E-PLP consumed after 1 min reaction

Amino-acid	1 mM	0.1 mM	Amino-acid	1 mM
Tyr	9		Leu	11
Phe	57		Val	0
Trp	0		Asp	0
His	88	25	Glu	4
Met	100	80	Arg	0

3. Results and discussion

3.1. Overall structure

The structure of YbdL was determined to 2.35 Å resolution with molecular replacement. As expected from the V_m, the asymmetric unit contains a dimer of $2 \times 45\,647$ Da. The electron density maps are of good quality, including the electron density for the bound cofactor pyridoxal-5-phosphate (Fig. 1).

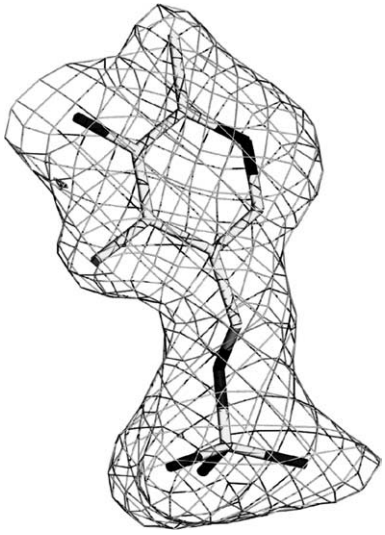

Fig. 1. Electron density map of PLP in the active site of YbdL. The final 3Fo-2Fc map has been contoured at 1σ-level.

The model was refined to a crystallographic R-factor of 0.199 (R_{free} 0.225), with a stereochemistry of the model as expected for this resolution (Table 1). Of a total of 386 residues for the native enzyme, the final model comprises residues 5–386 for each monomer, one pyridoxal phosphate molecule per monomer, and 251 water molecules.

Structure and sequence comparisons to other PLP enzymes (see below) identify YbdL as a member of subclass I of fold type I enzymes [4]. The structure analysis reveals that YbdL is structurally close to aspartate aminotransferase [5] with a rmsd value of 1.7 Å. Each enzyme subunit consists of two domains, a large domain (residues 50–329) containing a seven-stranded predominantly parallel β-sheet, surrounded by α-helices, and a small domain comprising residues 1–42 and 285–386 (Fig. 2B). The small domain folds into a three-stranded β-sheet (plus an elongated segment) covered with helices on one side.

The two subunits in the crystal asymmetric unit are related by a non-crystallographic dyad, resulting in the formation of a homodimeric molecule (Fig. 2A). The two active sites are located at the interface between the two subunits of the dimer, in a cleft formed by both domains of one subunit and the large domain of the second subunit and vice versa. This packing arrangement makes the dimer of YbdL the catalytically competent module (Fig. 2A), as is typical of this subclass of vitamin B_6 dependent enzymes.

3.2. Structural homologs

A search of the PDB data base using the program DALI [28] gives a number of similar structures, with the top solutions all being fold type I vitamin B_6 dependent enzymes. The closest

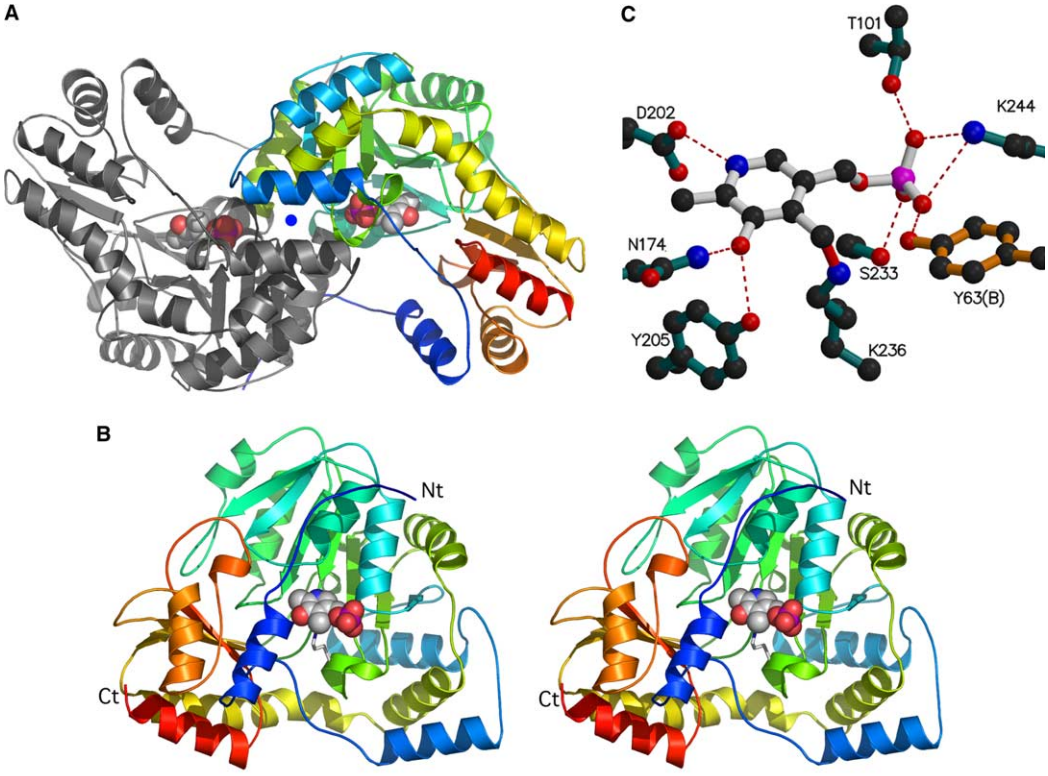

Fig. 2. Ribbon representation of YbdL. (A) View of the YbdL dimer with PLP as a space filling model in each monomer. The twofold axis is indicated by a blue circle. (B) Stereo ribbon view (rainbow coloration) of the monomer with the PLP in space filling mode covalently bound to lysine 236 (sticks). (C) View of the PLP molecule (ball-and-stick) in its binding pocket. The hydrogen bonds are represented by dashed lines. Views (A) and (B) made with PyMol [27]. View (C) made with Molscript [26].

structural relatives were aromatic amino acid aminotransferase from the hyperthermophilic archaeon *P. horikoshii* [16], *Z*-score 45.7, which was used for the molecular replacement solution, and aspartate aminotransferase from *Thermus thermophilus*, *Z*-score 45.7 [29]. They both display 30% amino acid identity with YbdL (Fig. 3). Structural superposition of YbdL with these two aminotransferases using the program O and default parameters gave rmsd values of 1.68 Å with 330 aligned Cα atoms for the *P. horikoshii* and 1.76 Å with 337 aligned Cα atoms for the *Th. thermophilus* enzyme, respectively.

3.3. Cofactor binding

In the cleft formed between the two domains of the subunit at the dimer interface, there is strong electron density adjacent to a conserved lysine residue, corresponding to a bound pyridoxal phosphate molecule (Fig. 1). No pyridoxal phosphate had been added during purification or crystallization, and it must therefore be bound to the enzyme already at the purification stage. PLP is covalently attached to YbdL via the ε-amino group of Lys236, a residue located at the N-terminus of a short helix following a β-strand. The phosphate group of PLP is anchored to the N-terminus of another α-helix, and forms hydrogen bonds to main chain nitrogen atoms of residues Ala100 and Thr101, and to the side chains of Tyr63, Thr101, Ser233, and Lys244. The aromatic ring of PLP packs against β-strands 3,5 and 5 of the central β-sheet. One side of the pyridine ring forms a stacking interaction with the side chain of Tyr125, the other side of the ring interacts with the side chains of Tyr205 and Val204. The nitrogen atom of the pyridine rings forms a hydrogen bond to the side chain of Asp202, an interaction found in all fold type I PLP enzymes [11].

3.4. Substrate binding site

Particularly noteworthy compared to aspartate aminotransferase [29] is the lack of the arginine residue at position 260 (corresponding to Arg292 in aspartate aminotransferase). An arginine residue at this position is typical of most aspartate aminotransferases and interacts with the distal carboxyl group of the aspartate substrate. It is thus an important determinant of specificity towards this amino acid. In some aspartate aminotransferases, a lysine residue at position 109 rather than Arg292 interacts with the carboxyl group of aspartate [29]. In YbdL, the corresponding residue is Thr101. The absence of basic residues characteristic of the aspartate binding site suggests that YbdL is not an aspartate aminotransferase.

This is further confirmed, since the closest relative to YbdL is an unusual aromatic aminotransferase from *Pyrococcus horikoshii* (Ph) with a novel specificity pattern towards α-amino acids [16]. While the enzyme has a preference for aromatic amino acids, it also is highly active with glutamic acid, but has very low affinity for aspartic acid. Typical structural features of this glutamic acid/aromatic amino transferase, which could explain this specificity profile, have been proposed based on a model of the enzyme – tyrosine and enzyme – glutamic acid complex. Several conserved hydrophobic amino acids are located in the substrate binding pocket of the enzyme. Almost all of these amino acids are conserved or functionally conserved in YbdL sequence (Fig. 3) and topology: Tyr 63 (B) (59 (B) in Ph), Tyr 125 (Phe 121 in Ph), Tyr 205 (202

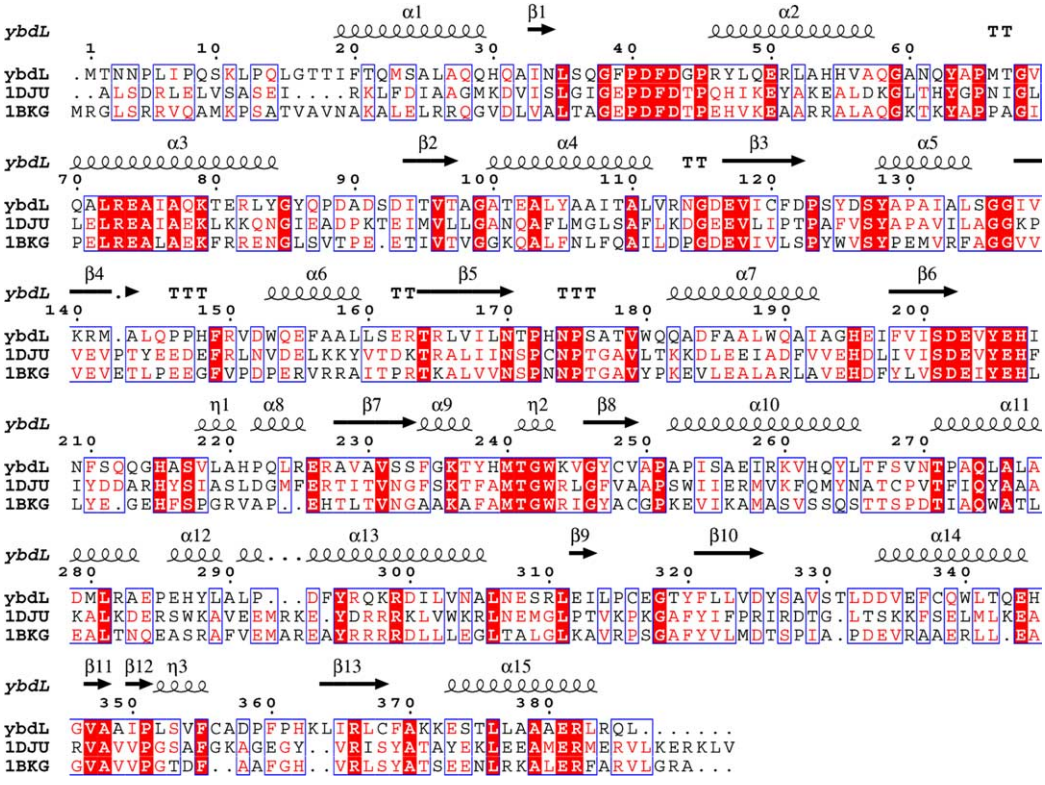

Fig. 3. Structure-based sequence alignment of YbdL from *E. coli*, an aromatic aminotransferase from *Pyrococcus horikoshii* (gi 15618406, 1DJU) [16] and aspartate aminotransferase from *Thermus thermophilus* (1BKG) [29]. The secondary structure elements for YbdL are shown. Both 1DJU and 1BKG display 30% sequence identity with YbdL.

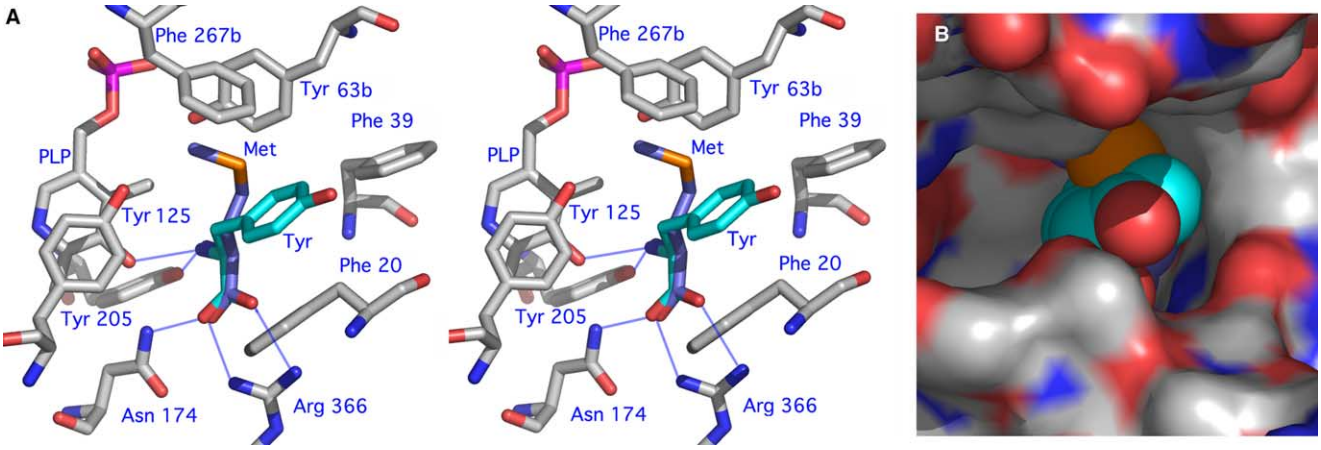

Fig. 4. Model of a Met or a Tyr ligand bound in the active site of YbdL. (A) Stereo view of the bound amino acids with residues of the active site. Ion/hydrogen bonds are represented by blue lines. (B) Molecular surface view of the model. Tyr and Met substrates are represented in space filling mode. Views made with PyMol [27].

in Ph), Phe 321 (Tyr 320 in Ph), Arg 366 (362 in Ph), Asn 174 (171 in Ph), Lys 144 (Arg 241 in Ph), while Phe 267 corresponds to a Threonine (254). The hydrophobic character of the binding pocket is thus comparable or higher than for the *Pyrococcus* enzyme, suggesting that YbdL should also have the capacity to bind aliphatic or aromatic amino acids.

3.5. Functional study

The amino transfer between two amino acids is a two steps reaction which can be summarized in the following scheme:

$$\text{PLP-enzyme} + \alpha\text{-amino acid 1} \Longleftrightarrow \text{PMP-enzyme} + \alpha\text{-keto acid1}$$

$$\text{PMP-enzyme} + \alpha\text{-keto acid 2} \Longleftrightarrow \text{PLP-enzyme} + \alpha\text{-amino acid2}$$

We have followed spectroscopically the first reaction with 10 amino acids: three aromatics (Trp, Phe, Tyr), three aliphatic (Leu, Met, Val), two acidic (Asp, Glu) one basic (Arg) and His (Table 2). The variation of OD at 430 nm was negligible in the presence of Trp, Val, Asp, and Arg, Methionine is the most active amino-donor. At 1 mM Met concentration, the reaction reaches 100% completeness almost immediately (in the time of mixing). At 0.1 mM, 80% completeness is reached in 1 min time. Reaction with His is also fast (Table 2), more than with Phe, Ala, Tyr, Leu and Glu. The final order of activity is therefore: Met > His > Phe > Tyr ~ Leu > Glu (Table 2).

3.6. Modelling study

We have modelled the binding of amino acids in the active site of YbdL using as a template the crystallographic complex of an aromatic amino acid transferase from *Paracoccus denitrificans* with 3-phenylpropionate [30]. Amino acids can be positioned in a comparable position, with their carboxylic group attached to Arg 366 and to Asn 174, replacing two water molecules (Fig. 4A). The NH2 leaving group is involved in two hydrogen bonds, with Tyr 205 OH group and with the O3 atom of PLP, in good position for transfer. The side chains are contained in a hydrophobic pocket delineated by PLP, Phe 20, Phe 39, Tyr 125, Tyr 63B and Phe 267B. Met or His could occupy the deeper part of the pocket, while Phe or Tyr would be turned slightly outside and would interact with all the above mentioned side-chains. Trp, instead, would clash with them, hence its absence of activity.

4. Conclusion

Ybdl belongs to subclass I of fold type I aminotransferases and contains a PLP bound molecule in the active site.. The precise function of YbdL in *E. coli* and YbdL homologs in other organisms has been assigned to a methionine aminotransferase. Modelization of amino acids in YbdL active site is in agreement with the activity study.

Acknowledgements: The ESRF is greatly acknowledged for beam time allocation. We thank the structural genomics team of the Marseille laboratory for technical assistance. This study was supported by the French Ministry of Industry (grant A.S.G.) and by the Genopoles project of the French Ministry of Education. It is a collaboration with the IGS laboratory and the Aventis company.

References

[1] Percudani, R. and Peracchi, A. (2003) A genomic overview of pyridoxal-phosphate-dependent enzymes. EMBO Rep. 4, 850–854.
[2] Grishin, N.V., Phillips, M.A. and Goldsmith, E.J. (1995) Modeling of the spatial structure of eukaryotic ornithine decarboxylases. Protein Sci. 4, 1291–1304.
[3] Jansonius, J.N. (1998) Structure, evolution and action of vitamin B_6-dependent enzymes. Curr. Opin. Struct. Biol. 8, 759–769.
[4] Schneider, G., Kack, H. and Lindqvist, Y. (2000) The manifold of vitamin B_6 dependent enzymes. Structure Fold Des. 8, R1–R6.
[5] Ford, G.C., Eichele, G. and Jansonius, J.N. (1980) Three-dimensional structure of a pyridoxal-phosphate-dependent enzyme, mitochondrial aspartate aminotransferase. Proc. Natl. Acad. Sci. USA 77, 2559–2563.
[6] Hyde, C.C. et al. (1988) Three-dimensional structure of the tryptophan synthase alpha 2 beta 2 multienzyme complex from *Salmonella typhimurium*. J. Biol. Chem. 263, 17857–17871.
[7] Shaw, J.P., Petsko, G.A. and Ringe, D. (1997) Determination of the structure of alanine racemase from *Bacillus stearothermophilus* at 1.9-Å resolution. Biochemistry 36, 1329–1342.
[8] Sugio, S. et al. (1995) Crystal structure of a D-amino acid aminotransferase: how the protein controls stereoselectivity. Biochemistry 34, 9661–9669.
[9] Weber, I.T. et al. (1978) Crystallographic studies on the activity of glycogen phosphorylase b. Nature 274, 433–437.

[10] Mehta, P.K. and Christen, P. (2000) The molecular evolution of pyridoxal-5′-phosphate-dependent enzymes. Adv. Enzymol. Relat. Areas Mol. Biol. 74, 129–184.
[11] Kack, H. et al. (1999) Crystal structure of diaminopelargonic acid synthase: evolutionary relationships between pyridoxal-5′-phosphate-dependent enzymes. J. Mol. Biol. 291, 857–876.
[12] John, R.A. (1995) Pyridoxal phosphate-dependent enzymes. Biochim. Biophys. Acta 1248, 81–96.
[13] Abergel, C. et al. (2003) Structural genomics of highly conserved microbial genes of unknown function in search of new antibacterial targets. J. Struct. Funct. Genomics 4, 141–157.
[14] Vincentelli, R. et al. (2003) Medium-scale structural genomics: strategies for protein expression and crystallization. Acc. Chem. Res. 36, 165–172.
[15] Sulzenbacher, G. et al. (2002) A medium-throughput crystallization approach. Acta Crystallogr. D: Biol. Crystallogr. 58 (Pt 12), 2109–2115.
[16] Matsui, I. et al. (2000) The molecular structure of hyperthermostable aromatic aminotransferase with novel substrate specificity from *Pyrococcus horikoshii*. J. Biol. Chem. 275, 4871–4879.
[17] Walhout, A.J. et al. (2000) GATEWAY recombinational cloning: application to the cloning of large numbers of open reading frames or ORFeomes. Methods Enzymol. 328, 575–592.
[18] Stura, E.A. et al. (1992) Crystallization of murine major histocompatibility complex class I H-2Kb with single peptides. J. Mol. Biol. 228, 975–982.
[19] Jancarik, J. et al. (1991) Crystallization and preliminary X-ray diffraction study of the ligand-binding domain of the bacterial chemotaxis-mediating aspartate receptor of *Salmonella typhimurium*. J. Mol. Biol. 221, 31–34.
[20] Matthews, B.W. (1968) Solvent content of protein crystals. J. Mol. Biol. 33, 491–497.
[21] Otwinowski, Z. (1993) in: DENZO: oscillation data and reducing program (Sawyer, L., Isaacs, N.W. and Bailey, S., Eds.), pp. 56–63, DLSCI/R34 Daresbury Laboratory, Warrington, UK.
[22] CCP4 and C.C.P.N. 4, 1994. The CCP4 suite: programs for crystallography. Acta Cryst. D 50, 760–766.
[23] Navaza, J. (1994) AMoRe: an automated package for molecular replacement. Acta Crystallogr. Sect. A 50, 157–163.
[24] Jones, T.A. et al. (1991) Improved methods for building protein models in electron density maps and the location of errors in these models. Acta Crystallogr. A 47 (Pt 2), 110–119.
[25] Brunger, A.T. et al. (1998) Crystallography & NMR system: a new software suite for macromolecular structure determination. Acta Crystallogr. D: Biol. Crystallogr. 54 (Pt 5), 905–921.
[26] Kraulis, P.J. (1991) MOLSCRIPT: a program to produce both detailed and schematic plots of protein structures. J. Appl. Crystallogr. 24, 946–950.
[27] W. DeLano (2004) The PyMOL Molecular Graphics System (http://www.pymol.org), San Carlos, CA, USA: DeLano Scientific LLC.
[28] Holm, L. and Sander, C. (1995) Dali: a network tool for protein structure comparison. Trends Biochem. Sci. 20, 478–480.
[29] Nakai, T. et al. (1999) Structure of *Thermus thermophilus* HB8 aspartate aminotransferase and its complex with maleate. Biochemistry 38, 2413–2424.
[30] Okamoto, A. et al. (1998) Crystal structures of *Paracoccus denitrificans* aromatic amino acid aminotransferase: a substrate recognition site constructed by rearrangement of hydrogen bond network. J. Mol. Biol. 280, 443–461.